JOURNAL OF
Materials
CHEMISTRY

Determination of surface free energy components for heterogeneous solids by means of inverse gas chromatography at finite concentrations

V. I. Bogillo,[a] **V. P. Shkilev and A. Voelkel**[b]*†

[a] *Institute of Surface Chemistry of the Ukrainian National Academy of Sciences, Pr. Nauki 31, 252022 Kiev, Ukraine*

[b] *Institute of Chemical Technology and Engineering, Poznań University of Technology, Pl. M. Skłodowskiej-Curie 2, 60–965 Poznań, Poland*

The approach for calculating the adsorption free energy and adsorption energy distributions for a heterogeneous solid surface as the sum of two uniform functions directly from co-ordinates of the tail of the probe's chromatographic peak is presented and discussed. Distribution functions are derived from data collected for the series of test adsorbates (*n*-alkanes C_5—C_{10} and five polar organic compounds) by means of inverse gas chromatography at finite concentrations. Average dispersive components of surface free energy and the donor/acceptor components of the adsorption energy in the monolayer region for the parent and mixed Si and Al pyrogenic oxides are also determined and discussed.

Introduction

The surfaces of most solids used as adsorbents, polymer fillers, catalysts and their supports are chemically and structurally heterogeneous. Surface properties are generally different to those of a bulk solid. Depending on the structures of the initial reactants, the preparation method and the pretreatment temperature, different types of adsorption sites may exist on a given surface. For example, several Brønsted and Lewis acid/base sites are the main types of active sites on the silica, titania, alumina and mixed (Si/Al) oxide surfaces. The properties of these sites depend strongly on their geometry, and display a distribution of the surface characterising parameters and its adsorption capacity.[1,2]

Inverse gas chromatography is one of the most convenient methods for the determination of the surface properties of powders.[3] This method allows the examination of a given material in terms of the surface free energy and acid/base characteristics of its surface.[4] When non-polar probes (*n*-alkanes) are used only London interactions exist between the adsorbate and the solid surface. The dispersive component of the surface free energy of any solid in the Henry region may be determined by measuring adsorption free energies for *n*-alkanes. This method has been applied in the examination of several inorganic oxides, polymers and fibres.[5] However, this approach is valid only for systems having a linear adsorption isotherm. In the case a of heterogeneous solid surface, the recorded chromatographic peaks are strongly asymmetrical, even for the low volumes of the injected liquid probe. They are typical for non-ideal, non-linear chromatography and are not suitable for measurements of the dispersive increment of the surface free energy and its donor/acceptor characteristics (*i.e.* acid/base properties). During investigation of the adsorption equilibrium at low coverage of a heterogeneous surface, the most active sites will be covered first. These sites correspond only to the initial part of the adsorption isotherm and they are not representative of all of the active sites. Therefore, the components of the surface free energy determined by the use of extremely low volumes of the test probes are related only to those strongest (and highly energetic) adsorption sites, which form only a small fraction of all active sites. Owing to the surface energetic heterogeneity, the correct parameters of surface adhesive ability in the monolayer region should be distributions on the dispersive and donor/acceptor components of the surface free energy and their initial moments, rather than the parameters related to the Henry region.

The aim of the present paper is the development of an approach for the determination of the components of the surface free energy, characterising the ability of a heterogeneous solid surface to take part in donor–acceptor and dispersive interactions. This approach is based on data collected by means of inverse gas chromatography at finite concentrations for a series of organic probes possessing different polarizability and acid/base properties. The proposed procedure is applied to characterization of the parent and mixed Si and Al pyrogenic oxides surfaces in their monolayer region.

Experimental

Materials

The following HPLC grade compounds (Aldrich) were used as test adsorbates: non-polar compounds: *n*-pentane, *n*-hexane, *n*-heptane, *n*-octane, *n*-nonane, *n*-decane; polar compounds: acetonitrile, ethyl acetate, chloroform, ethyl alcohol, and isopropyl alcohol. The characteristics of the test adsorbates used in the calculations of dispersive components of the surface free energy of the solids and the donor/acceptor components of their adsorption energy are listed in Table 1.

The pyrogenic parent and mixed Si and Al oxides were

Table 1 Molar deformation polarization (P_D), donor (DN) and acceptor (AN and AN*) numbers of test compounds

compound	P_D/cm^3	DN/ kcal mol^{-1}	AN	AN*/ kcal mol^{-1}
n-pentane	249.0	0	0	0
n-hexane	297.4	0	0	0
n-heptane	245.5	0	0	0
n-octane	391.6	0	0	0
n-nonane	438.2	0	0	0
n-decane	483.1	0	0	0
acetonitrile	110.5	14.1	18.9	41.7
ethyl acetate	221.0	17.1	9.3	1.5
chloroform	212.5	4	25.1	5.4
ethyl alcohol	127.4	20	37.9	10.3
isopropyl alcohol	184.3	29	33.0	3.1

---

† E-mail: voelkel@fct.put.poznan.pl

synthesized by Chlorovinyl Co. (Kalush, Ukraine) in joint flame hydrolysis of their chlorides. These oxides were used as chromatographic supports in the present study: silica sample (Aerosil 175) with a specific adsorption area measured by the BET method (low-temperature nitrogen adsorption) $S_A = 170 \pm 15\ m^2\ g^{-1}$, alumina sample ($S_A = 140 \pm 12\ m^2\ g^{-1}$) and mixed alumina–silica containing 30 wt.% Al in a silica matrix with $S_A = 170 \pm 16\ m^2\ g^{-1}$.

IGC experiments

The gas chromatographic measurements were carried out with the use of an LHM-80 gas chromatograph (Russia), equipped with a katharometer detector. The analog output from the detector was digitalized and recorded on an IBM PC 386 microcomputer controlled by original software (Turbo Pascal 7.0). Helium was used as the carrier gas. Air, as a non-interacting marker, was used to measure the dead volume of the column. Injection of the test compounds was repeated at least three times. Flow rate was measured at the end of the column with a bubble flow meter and its value was maintained at 20 cm^3 min^{-1}. Pressure measured at the inlet and outlet of the column was used to calculate the net retention volume by the usual procedure.[6] The molecular probes were injected manually with a Hamilton microsyringe (Hamilton microliter 700 and 7000 series syringe). The volume of injected liquid probe varied from 0.5–10 µl.

The examined solids were agglomerated, crushed and sieved to give particles 200–320 µm in size and placed in the chromatographic column (stainless steel, 40 cm long, 4 mm i.d.). The columns were conditioned under helium at 200 °C for 12 h before their use. The chromatographic measurements were carried out at temperature varying from 120–170 °C (isothermal conditions) with an increment of 10 °C. The temperature of the detector and sampler was 200 °C.

Calculation of primary data

Adsorption free energy distribution (or adsorption energy distribution) parameters were calculated immediately from the profile of the tail of the chromatographic peak at constant temperature and adsorbate amount (5 µl). Calculation of adsorbate pressure in the gas phase and saturated vapour pressure at the temperature of the experiment was performed with the use of Antoine's equation.[6] The cross-sectional area of adsorbate molecules on the flat surface was estimated using their liquid densities at 298 K, assuming a spherical molecular shape in a hexagonal close-packed configuration, or by using critical volumes of the test adsorbates.[7] Surface coverage was determined directly from the injected amount, the height of the peak, the area of the chromatographic peak, the cross-sectional area of the probe, the specific adsorption area of the chromatographic support and the amount of probe in the column.[6]

Results and Discussion

Determination of the adsorption free energy distribution directly from the parameters of the chromatographic peak

The 'multiple injection' and 'one-peak' methods are commonly applied to the analysis of the chromatographic peak dependence on the known amount of the liquid probe injected into the chromatographic column, and for the following determination of the adsorption isotherm on the surface of the chromatographic support.[6] In the first method a given amount of solute is injected quickly, inducing a peak. Adsorption or desorption may be followed by a mathematical examination of the front and tail of the recorded peak. The amount of the solute adsorbed onto the solid surface can be calculated as follows:

$$q = k\frac{D}{m}\int_0^h (t - t_0)\mathrm{d}h \qquad (1)$$

where q is the adsorbed amount per gram of adsorbent, D is the corrected flow of gas through the column, m is the weight of adsorbent in the column, t_0 and t are the retention times corresponding to the air peak and to the maximum of the solute peak, respectively, k is a proportionality coefficient between the height of the peak, h, and the corresponding concentration, c, of the solute in the gas phase ($k = c/h$). The concentration c is given by:

$$c = \frac{hq_m}{DS_{peak}} \qquad (2)$$

where S_{peak} is the area of the chromatographic peak and q_m is the injected amount of the test solute.

Eqn. (1) is valid if the temperature and the carrier gas/probe volumetric rate are constant in the whole column. The conditions of the one-peak method are fulfilled when the tails of the peaks from several injections (at increasing probe concentration) superimpose. Therefore it is possible to use a single peak corresponding to the maximum concentration of the test solute in the detector. This single peak should be cut into i slices corresponding to i pressures and amounts of the test solute. Eqn. (1) and (2) may then be transformed into eqn. (3) and (4):

$$q_i = k\frac{D}{m}\int_0^h (t_i - t_0)\mathrm{d}h_i \qquad (3)$$

$$c_i = \frac{h_i q_m}{DS_{peak}} \qquad (4)$$

where t_i is the retention time for the point localized on the right side of the i-slice at its height h_i, *i.e.* on the peak's tail. The integration of eqn. (3) is performed from 0 to the maximum height, h, of the chromatographic peak.

Fig. 1 and 2 present the chromatographic peak of *n*-hexane on the alumina/silica surface at 130 °C and the adsorption isotherms obtained from sequential integration of the *n*-hexane peaks measured at three different temperatures, respectively. This peak is strongly asymmetrical and it does not relate to the adsorption in the Henry region. The *n*-hexane adsorption isotherms are convex relative to the adsorbate pressure axis. This isotherm shape corresponds to a stronger adsorbate/surface interaction in comparison with attractive interactions between adsorbate molecules on the surface. Usually, the

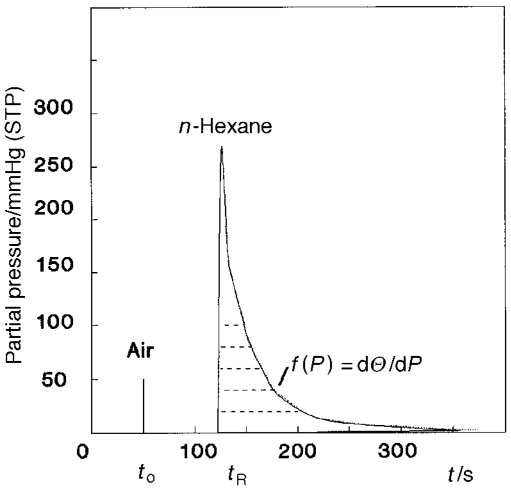

Fig. 1 Profile of the chromatographic peak of *n*-hexane on the alumina/silica surface at 403 K

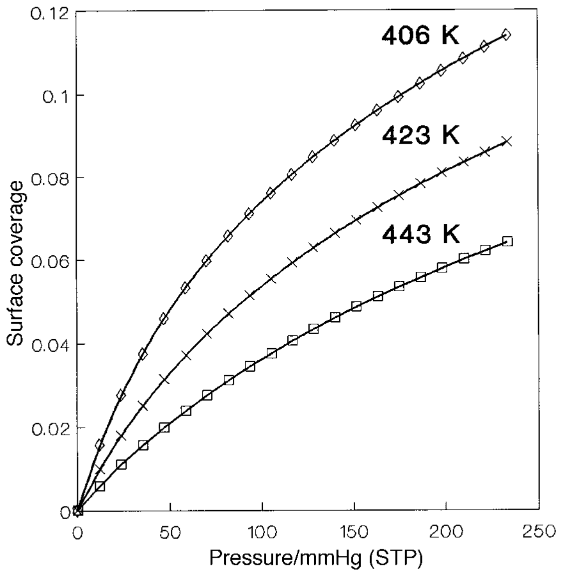

Fig. 2 Adsorption isotherms of *n*-hexane on the alumina/silica surface derived from the peak profiles recorded at three different temperatures

determination of the adsorption energy distribution from the chromatographic peak parameters requires the approximation of its co-ordinates by suitable polynomials or by spline functions and subsequent sequential integration of the peak's slices. This leads to the accumulation of numerical errors and to an increase of the distribution function uncertainty. Therefore we propose a simple direct analytical procedure for the calculation of the adsorption free energy distribution directly from the co-ordinates of the peak's tail.

As shown in Fig. 1, the following relationship can be evaluated immediately from the co-ordinates of the tail of the peak recorded in the chromatographic experiment

$$\frac{d\Theta}{dP}=f(P) \tag{5}$$

where Θ and P are the relative surface coverage and the adsorbate vapour pressure in the gas phase respectively. The common integral equation of the adsorption on the heterogeneous solid surface at isothermal conditions, assuming the Langmuir isotherm for the local surface coverage, may be presented as follows:[8]

$$\Theta(P,\ T)=\int_0^{\infty}\frac{(K_0)^{-1}\exp(E/RT)}{[1+(K_0)^{-1}\exp(E/RT)]}\chi(E)dE \tag{6}$$

where $\Theta(P, T)$ is the overall surface coverage at temperature T and adsorbate vapour pressure P, $\chi(E)$ is a normalized differential distribution function of the surface of adsorption energy E, K_0 is the Langmuir constant, R is the universal gas constant. The Langmuir constant may be estimated by using the Jaroniec equation:[9]

$$K_0=P_S\exp(\Delta H_{vap}/RT) \tag{7}$$

where ΔH_{vap} is the heat of evaporation of the adsorbate and P_S is its saturated vapour pressure at temperature T.

Let us substitute in eqn. (6) the distribution function of E $[\chi(E)]$ by a distribution function $[\rho(x)]$ of the following variable $x=E/RT-\ln(K_0)$. This equation is then transformed to:

$$\Theta(P,\ T)=\int_0^{\infty}\frac{P\exp(x)}{1+\exp(x)}\rho(x)dx \tag{8}$$

These functions are related by the simple expression:

$$\chi(E)=RT\rho(x) \tag{9}$$

The distribution function $\rho(x)$ may be presented as a stepped function including the sum of two uniform distribution functions $\rho_1(x)$ and $\rho_2(x)$ with joint first initial moment:

$$\rho(x)=\alpha\ \rho_1(x)+(1-\alpha)\rho_2(x) \tag{10}$$

where $0\leqslant\alpha\leqslant1$ and $\rho_1(x)$, $\rho_2(x)$ are defined as follows:

$$\rho_1(x)=\begin{cases}\dfrac{1}{x_2-x_1} & \text{at } x_1<x<x_2\\ 0 & \text{at } x<x_1;\ x>x_2\end{cases}\quad\text{and}$$

$$\rho_1(x)=\begin{cases}\dfrac{1}{x_4-x_3} & \text{at } x_3<x<x_4\\ 0 & \text{at } x<x_3;\ x>x_4\end{cases} \tag{11a}$$

The limits of these distributions are related by the following inequality:

$$x_1<x_3<x_4<x_2 \tag{11b}$$

The analytical solutions of eqn. (8) and for the derivative of the adsorption isotherm in terms of eqn. (10) and (11) may be written as follows:

$$\Theta(P,\ T)=\frac{\alpha}{x_2-x_1}\ln\left\{\frac{1+P\exp(x_2)}{1+P\exp(x_1)}\right\}+\frac{1-\alpha}{x_4-x_3}\ln\left\{\frac{1+P\exp(x_4)}{1+P\exp(x_3)}\right\} \tag{12}$$

and

$$\frac{d\Theta(P,\ T)}{dP}=\frac{\alpha}{x_2-x_1}\left\{\frac{\exp(x_2)}{1+P\exp(x_2)}-\frac{\exp(x_1)}{1+P\exp(x_1)}\right\}+\frac{1-\alpha}{x_4-x_3}\left\{\frac{\exp(x_4)}{1+P\exp(x_4)}-\frac{\exp(x_3)}{1+P\exp(x_3)}\right\} \tag{13}$$

All these values x_1, x_2, x_3, x_4 and α may be calculated by the least-mean-square method from an adsorption isotherm using eqn. (12), or from the co-ordinates of a chromatographic peak by using eqn. (13).

The next step in the procedure is the determination of the distribution cumulants, *i.e.* the average value (x_{av}) and its variance (σ_x^2) from values of the initial moments of the distribution on x:

$$x_{av}=M_1=\frac{\alpha(x_2+x_1)}{2}+\frac{(1-\alpha)(x_4+x_3)}{2} \tag{14a}$$

$$M_2=\frac{\alpha(x_2^3-x_1^3)}{3(x_2-x_1)}+\frac{(1-\alpha)(x_4^3-x_3^3)}{3(x_4-x_3)} \tag{14b}$$

$$\sigma_x^2=M_2-M_1^2 \tag{14c}$$

where M_2 and M_2 are the first and second initial moments of the distribution function on variable x.

The x_{av} values are related to the limits of the distribution (x_1, x_2, x_3, x_4) by simple expressions:

$$x_1=x_{av}-d_1 \tag{15a}$$

$$x_2=x_{av}+d_1 \tag{15b}$$

$$x_3=x_{av}-d_2 \tag{15c}$$

$$x_4=x_{av}+d_2 \tag{15d}$$

where d_1 and d_2 are the half-widths of the outer and inner uniform distribution functions $\rho_1(x)$ and $\rho_2(x)$, respectively.

The average (E_{av}) and the variance (σ_E^2) of the adsorption energy distribution $[\chi(E]$ are related to the above cumulants of the distribution function on x, as follows:

$$E_{av}=RTx_{av}+\ln(K_0) \tag{16a}$$

$$\sigma_E^2=(RT)^2\sigma_x^2 \tag{16b}$$

Using the above expressions one can calculate the limits of two distribution functions on E in eqn. (17a), similar to eqn. (10):

$$\chi(E)=\alpha\chi_1(E)+(1-\alpha)\chi_2(E) \qquad (17a)$$

$$\chi_1(E)=\begin{cases}\dfrac{1}{E_2-E_1} & \text{at } E_1<E<E_2\\ 0 & \text{at } E<E_1;\ E>E_2\end{cases}$$

$$\text{and } \chi_2(E)=\begin{cases}\dfrac{1}{E_4-E_3} & \text{at } E_3<E<E_4\\ 0 & \text{at } E<E_3;\ E>E_4\end{cases} \qquad (17b)$$

where $E_1<E_3<E_4<E_2$.

The limits of the function $\chi(E)$ (E_i, $i=1$–4) are related to the limits of the function $\rho(x)$ (x_i, $i=1$–4) by a simple relation:

$$E_i=RTx_i+\ln(K_0) \qquad (18b)$$

It is clear that the half-widths of the outer and inner uniform functions $\chi_1(E)$ (h_1) and $\chi_2(E)$ (h_2) coincide with those for functions $\rho_1(x)$ and $\rho_2(x)$ multiplied by RT: $h_1=RTd_1$ and $h_2=RTd_2$.

Then the adsorption energy distribution $\chi(E)$ may be calculated from eqn. (12)–(18) and eqn. (7)–(9). The Langmuir constant K_0 in the present study was calculated given the assumption that this value is independent of the type of solids and of the temperature within the temperature range used in our experiments (120–170 °C). Parameters for the adsorption free energy distribution function [$\Delta G_A=RT\ln(K_0)-E$], its average ($\Delta G_A{}^{av}$) and variance ($\sigma_{\Delta G_A}$) were calculated directly from eqn. (13)–(16) using the following expressions: $\rho(\Delta G_A)=\chi(E)$; $\Delta G_A{}^{av}=-RTx_{av}=RT\ln(K_0)-E_{av}$; $\sigma_{\Delta G_A}=\sigma_E{}^2$.

For example, the adsorption energy distribution calculated from the parameters of the *n*-hexane peaks' tail on the alumina/silica surface, at three different temperatures, as the sum of two uniform functions, is shown in Fig. 3. This distribution is equal to the reference one calculated from eqn. (12) with the use of adsorption isotherms.

As the exact computation of the five parameters (x_1, x_2, x_3, x_4 and α) by the least-mean-squares method requires highly accurate experimental points for the peaks' tail, the α value is assumed to be 0.5 in all our calculations. In such a case, the distributions $\rho(x)$ or $\chi(E)$ represent stepped functions including the sum of two uniform distribution functions $\rho_1(x)$ and $\rho_2(x)$ [or $\chi_1(E)$ and $\chi_2(E)$] with equivalent areas. It should be stated that the adsorption energy distribution, as the sum of two uniform distribution functions, was chosen in the present study to represent the possibility of the analytical solution of eqn. (8). Only a few analytical solutions are obtained for common integral equation of adsorption on the heterogeneous solid surface, containing simple local adsorption isotherms (Langmuir, Henry, Jovanovic) by using γ, exponential, Gaussian and two discrete distribution functions of the adsorption energy.[10–13] However, any of these functions may reflect the actual properties of the heterogeneous surface under investigation. From a mathematical point of view, eqn. (6) and (8) are Fredholm integral first-order equations. The solution of this equation with respect to $\rho(x)$ or $\chi(E)$ functions is a numerically ill-posed problem, *i.e.*, small changes in the measured adsorption $\Theta(P, T)$ caused by experimental errors may significantly distort the sought function. One of most suitable numerical methods for solving this ill-posed problem is the regularization procedure.[14] The number and areas of the peaks in the distribution curve obtained using this method can, in principle, reflect the number of different types of adsorption sites, their actual concentrations and adsorption potentials on the heterogeneous surface. For example, two peaks are exhibited in the adsorption energy distribution curves for diethyl ether and *n*-pentane on hydroxylated and trimethylsilylated silica surfaces.[15] Two peaks are also observed in the adsorption energy distribution curves for methanol and dichloromethane on hydroxylated and octadecyldimethylsilylated silica surfaces.[16] The position and intensity of the peaks depend on the structure of the adsorbates and the solid surface under investigation. The above distribution curves are calculated using different modifications of the regularization procedure from the adsorption isotherms measured by the classical volumetric method[15] or by inverse gas chromatography.[16] The number of peaks is in contradiction with the possible difference in the number of site types on the hydrophilic and hydrophobic silica surfaces for adsorption of non-polar and polar organic molecules.[17]

The optimization of the regularization parameter is crucial for the sought-for adsorption energy distribution. This parameter is dependent on the relative experimental error. A very low value of the regularization parameter gives rise to spurious peaks, while too high a value over-smooths the distribution function. It was shown that two nearby peaks may be recovered well by this method only for simulated isotherms without experimental error. Even an error as low as 0.1% flattens sharp peaks and gives only a shoulder. Wide peaks may be recovered by this method almost independently of the number of experimental points and the error inherent in the input data. For example, two to three peaks in the adsorption energy distribution curve are evaluated from low-temperature nitrogen adsorption on the surfaces of different activated carbons which accounts for a relative experimental error of 0.01%. Characteristically, these distribution curves at a relative error of 1% present only one peak with a long tail.[18] As a rule, the relative experimental error for points on the adsorption isotherms which are determined by means of gas chromatography exceeds 1%. This means that only wide peaks may be well represented on the adsorption energy distribution curve from these data using the regularization procedure. Hence, any analytical method including such a wide distribution may be used in these calculations. It was shown that analytical solution of the Fredholm integral equations of the first order, including two uniform distributions of both radiative and non-radiative rate constants for bimolecular photoreaction kinetics on the heterogeneous surface, gives the apparent rate constant distribution, which is close to that calculated by the regularization method.[19] Therefore, as proposed in the present study, the adsorption energy distribution as the sum of two uniform

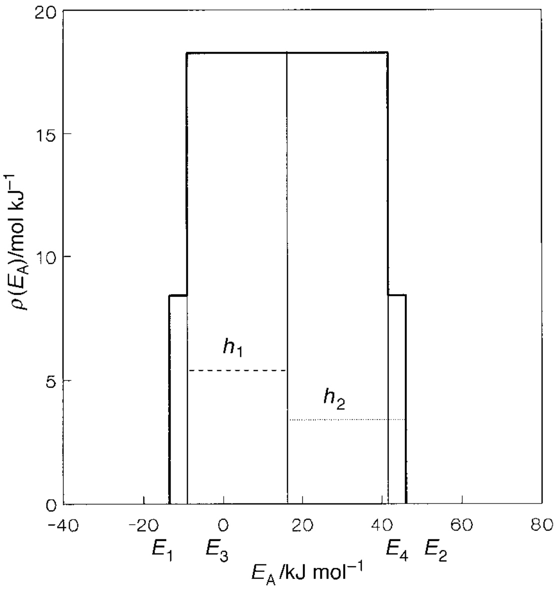

Fig. 3 The adsorption energy distribution function of *n*-hexane on the alumina/silica surface as the sum of two uniform functions calculated from parameters of the peaks tail recorded at three different temperatures

distribution functions is suitable for the description of adsorption data evaluated from chromatographic experiments with intermediate accuracy. Moreover, as the following calculations of dispersive and donor/acceptor components of the surface free energy for the heterogeneous solids require only knowledge of the first and second initial moments of the adsorption free energy distribution, the choice of such a simple distribution function possessing well defined limits is valid.

Determination of the dispersive component of the surface free energy in the monolayer region of heterogeneous solid

It was proposed to calculate the dispersive component of the surface free energy of a solid ($\gamma_S{}^d$) in the Henry region values of the adsorption free energy (ΔG_A) for *n*-alkanes series[4] obtained from gas chromatographic data (IGC)

$$\gamma_S{}^d = \frac{1}{4\gamma_{CH_2}}\left[\frac{\Delta G_A\,(CH_2)}{Na_{CH_2}}\right]^2 \tag{19}$$

where γ_{CH_2} is the surface energy of methylene group (35.6 mJ m^{-2} at 293 K). The variation of γ_{CH_2} with temperature is given by $\gamma_{CH_2} = 35.6 + 0.058(293 - T)$ (in mJ m^{-2}).[20] a_{CH_2} is the area occupied by a methylene group ($a_{CH_2} = 0.06$ nm^2). N is the Avogadro number and $\Delta G(CH_2)$ is the adsorption free energy of a methylene group.

Eqn. (19) may be transformed into the following relationship between the adsorption free energy at infinite dilution for the *n*-alkanes series and their carbon number (n)

$$-\Delta G_A = n2Na_{CH_2}\,(\gamma_S{}^d)^{1/2}\,(\gamma_{CH_2})^{1/2} + b \tag{20}$$

where b is a constant depending on the surface area of the solid in the column and on the choice of a reference state of the adsorbed solutes. When we have to apply the linear eqn. (20) for the description of the adsorption equilibrium on the heterogeneous surface, we can use cumulants of the first ($\Delta G_A{}^{av}$) and second order ($\sigma_{\Delta G_A}{}^2$) for the adsorption free energy distribution [$\rho(\Delta G_A)$] in this expression.

As the term $2Na_{CH_2}\,(\gamma_{CH_2})^{1/2} = \varsigma$ does not depend on the surface coverage, the average value and variance of distribution on the $[\Delta G_A(CH_2)]^2$ value may be calculated from the relationships between the average adsorption free energy of *n*-alkanes ($\Delta G_A{}^{av}$) or its variance ($\sigma_{\Delta G_A}{}^2$) and the number of carbon atoms (n). These parameters may be determined from the following relationships

$$-\Delta G_A{}^{av} = n\varsigma^{-1}[\Delta G_A(CH_2)]_{av} + b_{av} \tag{21}$$

and

$$\sigma_{\Delta G_A}{}^2 = n^2\varsigma^{-2}/\sigma_{\Delta G_A(CH_2)} + \sigma_b{}^2 \tag{22}$$

where b_{av} and $\sigma_b{}^2$ are the average and variance of the constant b.

The average value for $\Delta G_A(CH_2)$, given as $[\Delta G_A(CH_2)]_{av}$ is related to the average value for $[\Delta G_A(CH_2)]^2$, given as $\{[\Delta G_A(CH_2)]^2\}_{av}$ by the simple relationship

$$\{[\Delta G_A(CH_2)]^2\}_{av} = \{[\Delta G_A(CH_2)]_{av}\}^2 + \sigma_{\Delta G_A(CH_2)}{}^2 \tag{23}$$

The average value for the dispersive component of surface free energy of a heterogeneous solid can be calculated by using eqn. (24)

$$(\gamma_S{}^d)_{av} = \varsigma^{-2}\{[\Delta G_A(CH_2)]^2\}_{av} \tag{24}$$

It should be mentioned that the theory of multisite adsorption on the heterogeneous solid surface predicts the dependence of variance on the adsorption energy distribution for the *n*-alkanes series on the type of surface topography.[8] In the case of random topography of the surface sites this variance ($\sigma_E{}^2$ or $\sigma_{\Delta G_A}{}^2$) should increase with the increase in the number of carbon atoms in the *n*-alkane, whereas this is independent of the n value in the case of a patchwise surface topography. As a rule, real heterogeneous surfaces possess intermediate topography of the sites with a different correlation length between their adsorption energies.[8] Therefore, one can expect that the $\sigma_{\Delta G_A(CH_2)}{}^2$ value is equal to zero in the case of a patchwise surface topography and an increase in the case of a random site topography.

Determination of donor/acceptor components of adsorption energy in the monolayer region of a heterogeneous solid surface

Several attempts were made to evaluate the specific interaction parameters of surface free energy from the adsorption data of test compounds by means of IGC experiments at infinite dilution.[4,21,22]

By analogy with the method of calculation of specific interaction components of the adsorption heats of polar test adsorbates,[22] the average values of these components in the finite concentration region may be calculated by using the average values of the adsorption energy distributions for test nonpolar and polar probes.[23]

The average values of the adsorption energy distributions for polar test compounds may be presented as the sum of average values for the components of specific (donor–acceptor or hydrogen bonds) and non-specific (dispersive) interactions between the surface and adsorbates

$$E_{av} = E_{av}{}^{sp} + E_{av}{}^{nsp} \tag{25}$$

The energy of dispersive interactions between the large organic compound and the surface sites is proportional to the compound's molecular induced polarizability[22] or its molar deformation polarization (P_D)[1]

$$E_{av}{}^{nsp} = (K_P)_{av}P_D + \zeta \tag{26}$$

where the $(K_P)_{av}$ coefficient is proportional to the average polarizability of the surface adsorption sites and ζ is a constant characteristic for a given solid surface. The donor (DN) and acceptor (AN) numbers[24] describe the ability of the polar test solute to act as an electron donor and electron acceptor, respectively, in interactions with the surface active sites (acid/base parameters)

$$E_{av}{}^{sp} = \mathrm{AN}\frac{(K_D)_{av}}{100} + \mathrm{DN}\frac{(K_A)_{av}}{100} \tag{27}$$

where $(K_A)_{av}$ and $(K_D)_{av}$ coefficients denote the average ability of the surface sites to act as acceptor (electron acceptor or Lewis acid) and donor (electron donor or Lewis base) at interaction with the polar adsorbates. The quantities $(K_A)_{av}$ and $(K_D)_{av}$ are equal to the average acceptor and donor numbers of the surface sites.

The $(K_D)_{av}$ and ζ parameters may be determined by using values of the average adsorption energies for the *n*-alkanes series on the examined solid surfaces. The coefficients of eqn. (27) are easily determined by the least-squares method from the linear relationship for the series of polar adsorbates characterized by different DN and AN values

$$\frac{100E_{av}{}^{sp}}{\mathrm{AN}} = \frac{\mathrm{DN}}{\mathrm{AN}}(K_A)_{av} + (K_D)_{av} \tag{28}$$

However, different DN and AN scales for the test adsorbates are usually used for the evaluation of the donor–acceptor characteristics for solid surfaces from IGC data. For example, extended DN and AN scales calculated from the plot of the original DN Gutmann values *vs.* parameter B^* (shift of the valence vibration band of the OD group of deuteromethanol in the liquid under investigation) in accordance with the relation $\mathrm{DN} = -6.36 + 0.19B^*$ and from the plot of the original AN Gutmann values *vs.* E_T parameters (energy of the low electron transition of some betaine zwitterions) in accordance with the equation $\mathrm{AN} = -40.52 + 1.29E_T$,[25] were proposed in ref. 26. Riddle and Fowkes have shown that the ^{31}P NMR spectrum of triethylphosphine oxide, used in determining the

AN values for polar compounds, is appreciably shifted downfield due to van der Waals interactions with the solvents.[27] Hence, the AN values were corrected for the van der Waals contribution to the chemical shift on the basis of the determination of the γ^d values from the measurements of the surface and interfacial tensions of the test liquids. In many cases, this correction is quite substantial. The corrected AN values for polar test adsorbates are designated as AN*. The corrected $(K_D{}^*)_{av}$ values were determined from eqn. (29) by analogy to eqn. (28)

$$\frac{100E_{av}{}^{sp}}{AN^*}=\frac{DN}{AN^*}(K_A{}^*)_{av}+(K_D{}^*)_{av} \qquad (29)$$

Usually, one can also take into account the variances in donor ($\sigma_{K_D}{}^2$) and acceptor ($\sigma_{K_A}{}^2$) numbers of the heterogeneous surface. In accordance with the theorem of probability theory,[21] the common expression for these variances may be written as follows

$$\sigma_E{}^2=P_D{}^2\sigma_{K_P}{}^2+\left(\frac{AN}{100}\right)^2\sigma_{K_D}{}^2+\left(\frac{DN}{100}\right)^2\sigma_{K_A}{}^2+\sigma_\zeta{}^2 \qquad (30)$$

where $\sigma_{K_P}{}^2$ and $\sigma_\zeta{}^2$ are the variances of distributions on the K_P parameter of the surface and on the constant ζ, respectively.

Components of the surface free energy and adsorption energy of Si and Al pyrogenic oxides

The above approach was applied to the calculation of the adsorption energy distributions for *n*-alkanes series and different polar organic compounds and to estimate the average values of distribution functions and on the dispersive component of surface free energy as well as those for the donor/acceptor components of the adsorption energy distributions in the monolayer region. These parameters were determined for pyrogenic parent and mixed Si and Al oxide surfaces.

The half widths of two uniform distribution functions, average adsorption energies of the test solutes and their mean-square deviations at $\alpha=0.05$ on the surfaces of the examined oxides are presented in Tables 2–4.

Variance of the adsorption free energy distribution for the studied adsorbate/surface systems changes from 0.5 to 14 kJ^2 mol^{-2}. These high values of the variance are due to the considerable energetic heterogeneity of the oxide surfaces. No significant change in the variance of adsorption free energy for *n*-alkanes series on their carbon number was found. Therefore, it was assumed that $\sigma_{\Delta G_A(CH_2)}{}^2\approx 0$ in the eqn. (23) for all studied inorganic oxides. This is in accordance with predictions of the multisite adsorption theory on the heterogeneous surface.[8] The above value indicates in our case patchwise rather than random topography of the surface sites of the examined inorganic oxides. The values of the average dispersive component of surface free energy of these surface sites in the monolayer region were determined by using eqn. (23) from the squares of average values $[\Delta G_A(CH_2)]_{av}$. The average adsorption free energy for *n*-alkanes series on the examined oxides are presented in Table 5.

Table 2 Half widths of two uniform distribution functions (h_1 and h_2), the average adsorption energy (E_{av}) and its mean-square deviation (σ_E) (in kJ mol^{-1}) at $\alpha=0.05$, calculated from adsorption of the test solutes on the pyrogenic silica surface

adsorbate	h_1	h_2	E_{av}	σ_E
n-pentane	39.5	23.1	64.0	18.7
n-hexane	27.4	20.6	65.6	14.0
n-heptane	19.1	7.5	67.0	8.3
n-octane	20.9	12.9	69.4	10.0
n-nonane	19.4	11.1	70.7	9.1
n-decane	27.1	18.7	71.9	13.4
acetonitrile	31.3	30.0	71.4	17.7
ethyl acetate	25.3	18.3	72.6	12.8
chloroform	17.0	0.0006	66.1	6.9
ethyl alcohol	51.2	27.7	84.1	23.4
isopropyl alcohol	21.2	12.1	84.4	10.0

Table 3 Half widths of two uniform distribution functions (h_1 and h_2), the average adsorption energy (E_{av}) and its mean-square deviation (σ_E) (in kJ mol^{-1}) at $\alpha=0.05$, calculated from adsorption of the test solutes on the pyrogenic alumina surface

adsorbate	h_1	h_2	E_{av}	σ_E
n-pentane	24.2	19.1	67.0	12.6
n-hexane	40.9	7.0	70.6	16.7
n-heptane	13.0	0.001	75.0	5.3
n-octane	12.2	0.0013	79.4	5.0
n-nonane	12.8	0.0013	82.7	5.2
n-decane	14.4	2.53	84.9	6.0
acetonitrile	87.7	2.66	84.4	35.8
ethyl acetate	21.0	11.7	79.6	9.8
chloroform	12.9	0.0018	74.1	5.3
ethyl alcohol	28.6	20.8	91.1	12.0
isopropyl alcohol	17.4	8.8	90.4	7.8

Table 4 Half widths of two uniform distribution functions (h_1 and h_2), the average adsorption energy (E_{av}) and its mean-square deviation (σ_E) (in kJ mol^{-1}) at $\alpha=0.05$, calculated from adsorption of the test solutes on the pyrogenic alumina/silica surface

adsorbate	h_1	h_2	E_{av}	σ_E
n-pentane	21	2.6	59.0	13.6
n-hexane	29.8	25.0	62.6	16.0
n-heptane	25.1	18.0	68.0	12.8
n-octane	15.1	4.5	72.4	6.4
n-nonane	10.8	0.022	76.7	4.4
n-decane	7.32	0.0005	80.9	3.0
acetonitrile	14.3	6.2	81.4	6.4
ethyl acetate	21.0	9.4	81.6	9.5
chloroform	18.4	10.8	66.1	8.7
ethyl alcohol	22.7	17.5	92.1	11.7
isopropyl alcohol	27.0	18.1	88.4	14.2

The linear relationships between the average adsorption free energy of *n*-alkanes and their carbon numbers for the oxide surfaces are shown in Fig. 4. We calculated the average increment of the adsorption free energy of the methylene group, dispersive component of the surface free energy, specific components of the adsorption energy of polar adsorbates (Table 6) as well as average acceptor and donor numbers for the adsorption sites of these oxides. These data are presented in Table 7. The plots of average specific components of the adsorption energy for test polar compounds on the oxide surfaces *vs.* their DN/AN or DN/AN* ratios in the co-ordinates of eqn. (28) and (29) are shown in Fig. 5(a) and (b).

The average dispersive components of the surface free energy of pyrogenic inorganic oxides (Table 7) decrease in the following order: alumina > alumina/silica > silica. The dispersive component of the surface free energy is proportional to the overall polarizability of the surface sites, their ionization energy and to maximum partial charges on the atoms of these sites. The above sequence may be explained by the presence of very

Table 5 Average values of the adsorption free energy ($\Delta G_A{}^{av}$, in kJ mol^{-1}) at 403 K of *n*-alkanes on the surfaces of pyrogenic parent and mixed Si and Al oxides, calculated at $\alpha=0.05$

adsorbate	SiO_2	Al_2O_3	Al_2O_3/SiO_2
n-pentane	13.0	5.0	6.7
n-hexane	12.6	1.5	4.5
n-heptane	10.0	−1.8	1.1
n-octane	5.4	−4.4	0.35
n-nonane	3.1	−7.0	−3.1
n-decane	2.3	−9.5	−3.8

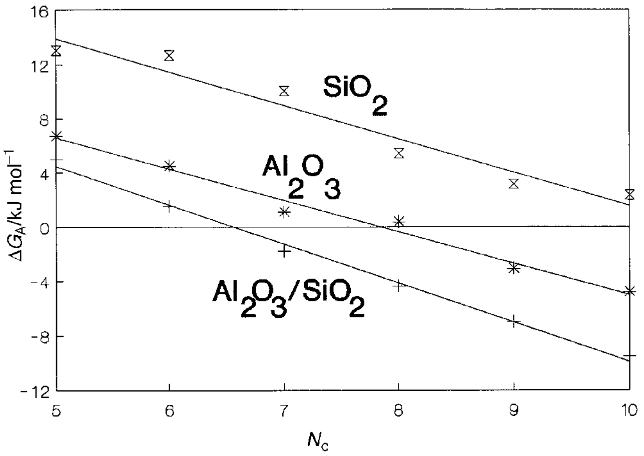

Fig. 4 Relationships between the average values of the adsorption free energy and the carbon number of *n*-alkanes on the pyrogenic parent and mixed Si and Al oxide surfaces at 403 K

Table 6 Average specific interaction components of the adsorption energy (E_{av}^{sp}, in kJ mol^{-1}) of polar test compounds on the surfaces of parent and mixed Si and Al pyrogenic oxides

compound	SiO_2	Al_2O_3	Al_2O_3/SiO_2
acetonitrile	12.3	28.2	36.0
ethyl acetate	9.6	14.7	25.6
chloroform	3.4	9.8	10.9
ethyl alcohol	24.4	33.6	45.0
isopropyl alcohol	22.7	28.4	35.9

Table 7 Average values of the increment of adsorption free energy for the methylene group ($[\Delta G_A(CH_2)]_{av}$, in kJ mol^{-1}), dispersive component of the surface free energy at 403 K [$(\gamma_S{}^d)_{av}$, in mJ m^{-2}], acidities [$(K_A)_{av}$ and $(K_A{}^*)_{av}$], basicities [$(K_D)_{av}$, in kcal mol^{-1} and $(K_D{}^*)_{av}$], relative acidities (K_A/K_D, mol kcal^{-1} and $K_A{}^*/K_D{}^*$) of the surfaces of pyrogenic parent and mixed Si and Al oxides, and correlation coefficients (*R*) of the relationships (21), (28) and (29)

parameter	SiO_2	Al_2O_3	Al_2O_3/SiO_2
$[\Delta G_A(CH_2)]_{av}$	2.15	2.89	2.29
$(\gamma_S{}^d)_{av}$	28.6	51.8	32.5
R for eqn. (21)	0.996	0.996	0.999
$(K_D{}^*)_{av}$	21.8 ± 7.8	46.7 ± 21.0	34.4 ± 25.9
$(K_A{}^*)_{av}$	11.7 ± 1.4	16.8 ± 3.8	32.9 ± 4.7
$K_A{}^*/K_D{}^*$	0.54	0.36	0.96
R for eqn. (29)	0.979	0.931	0.971
$(K_D)_{av}$	5.8 ± 2.8	12.4 ± 6.6	9.6 ± 8.0
$(K_A)_{av}$	11.2 ± 2.8	15.0 ± 6.6	30.9 ± 8.0
K_A/K_D	1.93	1.21	3.21
R for eqn. (28)	0.916	0.793	0.911

*In calculating these parameters the average specific component of adsorption energy was expressed in kcal mol^{-1} while DN and AN values were taken from ref. 24.

polar Brønsted acid sites and highly polarizable Lewis acid/base sites on the surfaces of alumina and mixed oxides containing Al in the silica matrix, in comparison to the parent silica.

Some difficulties exist when the $\gamma_S{}^d$ values from the present study are compared with those evaluated from IGC data at infinite dilution. It was reported that the $\gamma_S{}^d$ value for pyrogenic silica (Aerosil 130 from Degussa) equals 46.5 mJ m^{-2} at 383 K,[4] or 40 ± 4 mJ m^{-2} at 353 K.[28] These $\gamma_S{}^d$ values were obtained in Henry's region. It is known that $\gamma_S{}^d$ for initial and modified silicas decreases with the increasing temperature by 0.3–0.5 mJ m^{-2} °C^{-1}.[29] Much higher $\gamma_S{}^d$ values were reported for Aerosil 300 ($\gamma_S{}^d = 76$ mJ m^{-2} at 333 K, 67 mJ m^{-2} at 363 K and 68 mJ m^{-2} at 393 K)[30] and for Spherosil XOB 75 ($\gamma_S{}^d =$ 80 mJ m^{-2} at 293 K).[29] These values are related to the strongest adsorption sites on the silica surface. Increase of temperature and surface coverage causes a decrease in the $\gamma_S{}^d$ value. For example, estimates of $\gamma_S{}^d$ values at 293 K when the temperature coefficient of $\gamma_S{}^d$ from ref. 29 was taken into account and our $(\gamma^d{}_S)_{av}$ data at 403 K lead to $\gamma_S{}^d = 60$–80 mJ m^{-2}. Hence, the average dispersive component of the surface free energy of silica (28.6 mJ m^{-2} at 403 K) found in the present study may be treated as the true value of this parameter characterizing the overall popularity of the surface sites.

The dispersive component of the surface free energy for alumina samples depends on the modification (α- or γ-phases, boehmite), temperature of the pretreatment of the surface and on the content of silica and other oxides in their matrix. It was reported that γ-alumina pretreated at 473 K has higher $\gamma_S{}^d = 115$ mJ m^{-2} at 373 K, in comparison with Aerosil 200 ($\gamma_S{}^d = 65$ mJ m^{-2}) under the same conditions.[31] The boehmite (Al_2O_3, H_2O or AlOOH) is characterized by $\gamma_S{}^d = 172$ mJ m^{-2} at 353 K.[31] The $\gamma_S{}^d$ value for alumina samples decreases from 100 mJ m^{-2} to 65 mJ m^{-2} and to 42 mJ m^{-2} at 373 K with an increase in silica content from 45–630 ppm and to 1060 ppm in the alumina matrix.[32] Additionally, it was reported that $\gamma_S{}^d$ increased from 48 to 71 mJ m^{-2} for aluminas after their dry grinding.[33] Therefore, despite the large differences in the reported $\gamma_S{}^d$ values for silica, alumina and alumina/silica, one may conclude that the $\gamma_S{}^d$ value increases during the transition from silica to alumina samples and may decrease due to the increase of silica content in the alumina matrix. This conclusion fits well with our data for variation of $(\gamma_S{}^d)_{av}$ values for pyrogenic silica, alumina and alumina/silica samples.

No clear relationship was found between the variances for adsorption energy distribution of polar probes and squares of their donor or acceptor numbers (correlation coefficients were found to be below 0.5).

The electron donor ability or basicity of adsorption sites of the examined oxides in accordance with the change of their $(K_D)_{av}$ and $(K_D{}^*)_{av}$ values increases in the order: silica < alumina/silica < alumina and their electron acceptor ability or acidity, as it follows from their $(K_A)_{av}$ and $(K_A{}^*)_{av}$ values, varies as: silica < alumina < alumina/silica.

The ability of the inorganic oxide surfaces to interact with organic compounds as acid or as base can be estimated from the comparison of the mean electronegativities of these solids. The mean orbital electronegativity of a solid (χ_S) may be calculated from the following relationships[34]

$$\chi_S = \frac{\Sigma(n_i \chi_i)}{\Sigma n_i} \tag{31}$$

and

$$\chi_i = IP_i + EA_i \tag{32}$$

where χ_i, IP_i and EA_i are the Mulliken orbital electronegativity, first ionization potential and electron affinity of the *i*th atom in the inorganic molecule, respectively, while n_i is the number of these atoms in the molecule. The estimated χ_S values for alumina and silica are 5.82 eV and 6.61 eV, respectively. This means that acidic properties increase during the transition from alumina to silica, whereas the basic properties increase in the opposite direction. It is well known that bulk alumina exhibits basic properties during interaction with typical Brønsted acids, whereas silica typically displays acidic properties. This conclusion coincides with that observed in the present study of an increase of $(K_D)_{av}$ during the transition from silica to alumina. The surface of α-Al_2O_3 is characterized by a higher donor number ($K_D = 21$ kcal mol^{-1}) in comparison with its acceptor number ($K_A = 15$)[35] (data from inverse chromatography at infinity dilution and zetametry measurements). This agrees with the increase of basic properties, determined on the basis of its $(K_D)_{av}$ and $(K_A)_{av}$ values in the present study, on changing from silica to alumina samples.

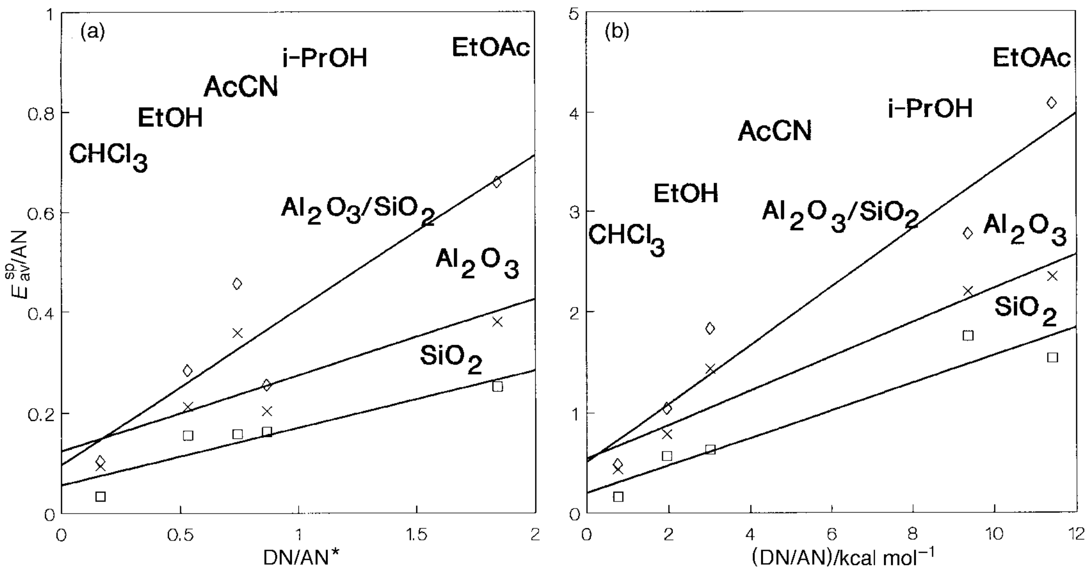

Fig. 5 Plots of the average specific components of the adsorption energy for test polar compounds on the parent and mixed Si and Al pyrogenic oxide surfaces *vs.* (a) their DN/AN ratio [eqn. (28)] and (b) their DN/AN* ratio [eqn. (29)]

It is known that OH groups of the alumina surfaces display a wide range of Brønsted acidic and basic properties.[2] The single OH groups of the surfaces exhibit mainly typical basic properties, whereas the bridged OH groups bonded to trigonal aluminium atoms behave as typical Brønsted acid sites.[36]

It should be mentioned that the behaviour of such main active sites as OH groups at the oxide surfaces depends strongly on the composition of the oxide and the local chemical environment. On partially dehydroxylated surfaces they have varying acid/base character and interact with adsorbates according to acid/base characteristics, such as ionization potential, electron affinity, proton affinity and partial charges on the atoms in the surface cluster. The comparison of the positive charges on the OH groups and lengths of the OH bonds in the surface clusters of possible OH groups on the silica, alumina and alumina/silica surfaces leads to the conclusion that the acidity of these groups decreases in the transition from alumina/silica to alumina and to silica.[36] Recent quantum chemical computations have shown that the main Brønsted acidic sites of silica are single and geminal OH groups, whereas those of binary alumina/silicas are bridged OH groups and water molecules coordinated on a trigonal aluminium atom.[36,37] The observed enhancement of acidic characteristics for the mixed alumina/silica compared with the parent Al and Si oxides may be explained in terms of the formation of strong Lewis acidic sites and by enhancement of the acidity of OH groups which are bound to the aluminium cations on the boundaries between Al_2O_3 patches and the SiO_2 lattice.[38]

The average acidity of the oxide surfaces, which can be estimated as the K_A/K_D ratio, depends on the choice of acceptor number (AN or AN*) (Table 7). When the AN values are used, *i.e.* acceptor properties of the test adsorbates are overestimated, the relative acidity of all examined oxides is less than one, *i.e.* they exhibit basic rather than acidic properties. Their relative acidity decreases in the following order: alumina/silica > silica > alumina. This order is not changed when the AN* values for polar adsorbates accounting for the contribution of van der Waals interactions are used. However, in this case (Table 7) the relative acidity of the oxides is more than one, *i.e.* they exhibit acidic rather than basic properties. Therefore, application of the AN* values in the calculations of the acid/base properties of the solid surfaces results in the increase of their relative acidity.

Conclusions

The approach was proposed for the calculation of the adsorption free energy distribution and the parameters describing donor–acceptor and dispersive properties for heterogeneous solid surfaces. The calculations were carried out with the use of chromatographic data for a peak profile measured at finite adsorbate concentrations. Moreover, the average dispersive and donor–acceptor components of surface free energy for a heterogeneous solid in the monolayer region may be obtained by the use of the proposed procedure. These parameters seem to be the most appropriate characteristics of adhesion ability for a heterogeneous solid surface. The calculations of such parameters were performed for adsorption sites on the surfaces of parent and mixed Si and Al pyrogenic oxides. It was found that the surface adsorption sites of mixed alumina–silica exhibit a highly acidic character in comparison to the parent oxides.

This work was partially supported by PUT grant DS 32/265/97.

References

1 V. I. Bogillo, A. S. Semenyuk and E. V. Utlenko, *Ukr. Khim. Zh. (Russ. Ed.)*, 1994, **60**, 398.
2 H. Knozinger and P. Ratnasamy, *Catal. Rev. Sci. Eng.*, 1978, **17**, 31.
3 *Inverse Gas Chromatography. Characterization of Polymers and Other Materials*, ed. D. R. Lloyd, T. C. Ward and H. P. Schreiber, ACS Symp. Ser. No. 391, American Chemical Society, Washington DC, 1989.
4 C. Saint Flour and E. Papirer, *Ind. Eng. Chem. Prod. Res. Dev.*, 1982, **21**, 666.
5 A. Voelkel, *Crit. Rev. Anal. Chem.*, 1991, **22**, 411.
6 R. C. Reid, J. M. Prausnitz and T. K. Sherwood, *The Properties of Gases and Liquids*, McGraw-Hill, New York, 1977.
7 J. R. Conder and C. L. Young, *Physicochemical Measurements by Gas Chromatography*, Wiley, New York, 1979.
8 W. Rudzinski and D. H. Everett, *Adsorption of Gases on Heterogeneous Surfaces*, Academic Press, New York, 1991.
9 M. Jaroniec, *Surf. Sci.*, 1975, **50**, 553.
10 S. Ross, *Adsorption Technol.*, 1971, **67**, 1.
11 J. Roles and G. Guiochon, *J. Chromatogr.*, 1992, **591**, 345.
12 J. A. Lum Wan and L. R. White, *J. Chem. Soc., Faraday Trans.*, 1991, **87**, 3051.
13 M. Jaroniec, X. Lu and R. Madey, *J. Phys. Chem.*, 1990, **94**, 5917.
14 A. M. Puziy, V. V. Volcov, O. I. Poznayeva, V. I. Bogillo and V. P. Shkilev, *Langmuir*, 1997, **13**, 1303.

15 V. I. Bogillo, V. P. Shkilev and G. R. Yurchenko, *Ukr. Khim. Zh.*, 1995, **61**, 318.
16 M. Pyda and G. Guiochon, *Langmuir*, 1997, **13**, 1020.
17 R. K. Iler, *The Chemistry of Silica*, Wiley Interscience, New York, 1979.
18 R. Leboda, J. Skubiszewska-Zieba and V. I. Bogillo, *Langmuir*, 1997, **13**, 1211.
19 V. I. Bogillo, V. P. Shkilev and V. V. Osipov, *Langmuir*, 1997, **13**, 945.
20 G. M. Dorris and D. G. Gray, *J. Colloid Interface Sci.*, 1980, **77**, 353.
21 J. Schultz, L. Lavielle and C. Martin, *J. Adhesion*, 1987, **23**, 45.
22 J. B. Donnet, S. J. Park and H. Balard, *Chromatographia*, 1991, **31**, 434.
23 G. A. Korn and T. M. Korn, *Mathematical Handbook for Scientists and Engineers*, Nauka, Moscow, 1968.
24 V. Gutmann, *The Donor-Acceptor Approach to Molecular Interactions*, Plenum Press, New York, 1978.
25 R. Schmidt and V. N. Sapunov, *Non-Formal Kinetics*, Verlag Chemie, Weinheim, 1982.
26 A. Vidal, E. Papirer, W. M. Jiao and J. Donnet, *Chromatographia*, 1987, **23**, 121.
27 F. L. Riddle, Jr. and F. M. Fowkes, *J. Am. Chem. Soc.*, 1990, **112**, 3259.
28 H. Haidar, H. Balard and E. Papirer, *Colloids Surf. A*, 1995, **99**, 45.
29 W. J. Wang, S. Wolff and J. B. Donnet, *Rubber Chem. Technol.*, 1991, **64**, 559.
30 E. Papirer, H. Balard, Y. Rahmani, A. P. Legrand, L. Facchini and H. Hommel, *Chromatographia*, 1987, **23**, 639.
31 E. Papirer, G. Ligner, H. Balard, A. Vidal and F. Mauss, in *Proc. Chemically Modified Surface Symp., Midland, Michigan, June 28–30, 1989*, ed. D. E. Leyden and W. T. Collins, Gordon and Breach, New York, 1989, pp. 15–26.
32 E. Papirer, J. M. Perrin, B. Siffert and G. Philipponneau, *Prog. Colloid Polym. Sci.*, 1991, **84**, 252.
33 E. Papirer, J. M. Perrin, B. Siffert, G. Philipponneau and J. M. Lamerant, *J. Colloid Interface Sci.*, 1993, **156**, 104.
34 V. I. Bogillo, *Composite Interfaces*, submitted.
35 B. Siffert, J. Eleli-Letsango, A. Jada and E. Papirer, *Colloids Surf.*, 1994, **92**, 107.
36 V. I. Bogillo and V. M. Gun'ko, *Langmuir*, 1996, **12**, 153.
37 G. M. Zhidomirov and V. B. Kazansky, *Adv. Catal.*, 1986, **34**, 131.
38 J. Sauer, *J. Mol. Catal.*, 1989, **54**, 312.

Paper 8/01703D; *Received* 2nd *March*, 1998